NeuroImage 111 (2015) 107–122

Contents lists available at ScienceDirect

NeuroImage

journal homepage: www.elsevier.com/locate/ynimg

Multi-contrast multi-scale surface registration for improved alignment of cortical areas

Christine Lucas Tardif [a,*], Andreas Schäfer [a], Miriam Waehnert [a], Juliane Dinse [a,b], Robert Turner [a], Pierre-Louis Bazin [a]

[a] Department of Neurophysics, Max Planck Institute for Human Cognitive and Brain Sciences, Leipzig, Germany
[b] Faculty of Computer Science, Otto-von-Guericke University, Magdeburg, Germany

ARTICLE INFO

Article history:
Accepted 2 February 2015
Available online 9 February 2015

Keywords:
Surface registration
Cortical alignment
T1
Myeloarchitecture
Multi-contrast
Symmetric diffeomorphic transformation

ABSTRACT

The position of cortical areas can be approximately predicted from cortical surface folding patterns. However, there is extensive inter-subject variability in cortical folding patterns, prohibiting a one-to-one mapping of cortical folds in certain areas. In addition, the relationship between cortical area boundaries and the shape of the cortex is variable, and weaker for higher-order cortical areas. Current surface registration techniques align cortical folding patterns using sulcal landmarks or cortical curvature, for instance. The alignment of cortical areas by these techniques is thus inherently limited by the sole use of geometric similarity metrics. Magnetic resonance imaging T1 maps show intra-cortical contrast that reflects myelin content, and thus can be used to improve the alignment of cortical areas. In this article, we present a new symmetric diffeomorphic multi-contrast multi-scale surface registration (MMSR) technique that works with partially inflated surfaces in the level-set framework. MMSR generates a more precise alignment of cortical surface curvature in comparison to two widely recognized surface registration algorithms. The resulting overlap in gyrus labels is comparable to FreeSurfer. Most importantly, MMSR improves the alignment of cortical areas further by including T1 maps. As a first application, we present a group average T1 map at a uniquely high-resolution and multiple cortical depths, which reflects the myeloarchitecture of the cortex. MMSR can also be applied to other MR contrasts, such as functional and connectivity data.

Introduction

Image registration is crucial for brain mapping studies, such as comparative morphometry and group analysis of functional data, in order to compensate for differences in position, size and shape of brain structures across individuals. Many fully automated non-linear volume registration algorithms have been developed to align brain structures, and produce very good results even for strong differences due to pathology (see Klein et al. (2009) for a review). Although these algorithms perform well for deep brain structures, they fail to accurately align the cerebral cortex, a thin sheet that is highly convoluted and variable. In magnetic resonance imaging (MRI) studies, surface registration, which aligns 2D manifolds based on their shape, is often preferred over volume registration to align cortical areas between subjects or with an atlas. The pioneering work of Brodmann (1909) and more recent histological studies (Fischl et al., 2008; Hinds et al., 2008) have shown that cortical folding patterns can be used to approximately predict the location of cortical areas, with the highest accuracy for primary cortical areas. Surface registration driven by cortical folding patterns also improves the statistical power and spatial specificity of group functional MRI analysis (Frost and Goebel, 2012; van Atteveldt et al., 2004) due to improved alignment of functional areas.

In spite of this significant improvement in cortical alignment, folding-based surface registration is inherently limited in two ways. There are regions of high inter-subject folding variability, defined in Ono's *Atlas of the Cerebral Sulci* (Ono et al., 1990), where the number of folds may differ and a one-to-one mapping of folds is not possible. Furthermore, the boundaries between functional cortical areas have a complex and variable relationship with the cortical folding pattern, in particular for higher cognitive and association cortex. Inter-subject variability in size and shape of the primary visual cortex in relation to sulcal folds has been shown in histology studies (Amunts et al., 2000; Hinds et al., 2008). More significant variability has been shown for non-primary areas including the motion sensitive visual complex MT+/V5 and Broca's area using histology (Fischl et al., 2008), task-based fMRI (Frost and Goebel, 2012), as well as T1-weighted/"T2-weighted" images (Glasser and Van Essen, 2011). Due to this complex relationship, the alignment of cortical areas is improved but is also inherently limited

* Corresponding author at: Max Planck Institute for Human Cognitive and Brain Sciences, Department of Neurophysics, Stephanstrasse 1A, 04301 Leipzig, Germany.
E-mail address: ctardif@cbs.mpg.de (C.L. Tardif).

http://dx.doi.org/10.1016/j.neuroimage.2015.02.005
1053-8119/

by the use of geometric information to drive the surface registration. Assuming a perfect alignment of the geometric similarity metric, such as curvature or sulcal landmarks, is achieved, there will remain a residual error in the alignment of cortical areas between subjects.

Cortical micro-architectonic features, such as the density, size, orientation and shape of cells and myelin sheaths, are more strongly related to cortical function than cortical folding patterns (Amunts et al., 2007). Structural MR images show myelin contrast that reflects the architectonic boundaries of cortical areas (Geyer et al., 2011). Very high-resolution T1 maps show exquisite intra-cortical contrast that varies as a function of cortical depth (Geyer et al., 2011; Lutti et al., 2014a; Tardif et al., 2013). Recent studies have mapped individual and group average T1 maps (Bazin et al., 2014; Sereno et al., 2013; Weiss et al., 2010), T2* maps (Cohen-Adad et al., 2012) and T1-weighted/"T2-weighted" images (Glasser and Van Essen, 2011) onto the cortical surface. Primary areas and extrastriate visual areas, which are densely myelinated, are clearly discernible on the inflated surfaces. These "myelin maps" have been shown to truly reflect the location of functionally specialized areas of the cortex using topological mapping fMRI (Bridge et al., 2005; Dick et al., 2012; Sereno et al., 2013), as well as task and resting-state fMRI (Van Essen and Glasser, 2014). We propose to use T1 maps, a quantitative index of primarily myelin content (Geyer et al., 2011; Stüber et al., 2014), to improve the surface-based alignment of cortical areas.

In this paper, we present a novel automated multi-contrast multi-scale surface-based registration technique (MMSR) for precise surface registration, with key improvements over current methods. MMSR applies a non-linear volume-based registration algorithm to surface information represented in volume space, rather than computing a deformation restricted to a spherical manifold. It can therefore be applied to surfaces with non-spherical topology, and the computed deformation is meaningful for statistical shape analysis (Miller, 2004). MMSR registers the level-set representation of the cortical surfaces and two curvature metrics (curvedness and shape index). We developed a multi-scale approach that is applied to a hierarchy of partially inflated level set surfaces with a shrinking narrowband. The final transformation is a direct symmetric diffeomorphic mapping between the original surfaces in volume space. MMSR was first introduced in a recent conference paper (Tardif et al., 2013). Here, we describe our improved implementation in detail.

For validation, we quantitatively compare MMSR to two widely accepted surface registration algorithms: FreeSurfer and Spherical Demons. Firstly, we build geometric group templates and calculate the group average and standard deviation of the registration metric, i.e. curvature, to compare the precision of the alignment. Secondly, we perform pairwise registration experiments of surfaces from the Mindboggle-101 dataset that have been manually labeled. The overlap of the labels after alignment is an indication of registration accuracy, i.e. whether the corresponding gyri have been aligned or the algorithm is sensitive to local minima.

MMSR can also include other contrasts instead of, or in addition to, the curvature metrics to drive the registration. We demonstrate this feature by including intra-cortical T1 contrast with the objective to improve the alignment of cortical areas. We present a unique high-resolution (0.5 mm isotropic) group-average T1 map of the cortical surface at four cortical depths.

Multi-contrast surface registration

The level-set framework

The MMSR algorithm applies non-linear volume registration to surface information represented in Cartesian space using a level-set framework. The level-set representation $\varphi(v)$ of a surface is a signed distance function, i.e. the value at voxel v is equal to the distance of voxel v from the surface, positive outside the surface and negative inside (Osher and Sethian, 1988). The level-set is often only defined within a maximum distance from the surface, a narrowband, to enhance computation efficiency. An example of a level-set volume image and the corresponding mesh of a cortical surface are shown in Fig. 1. Distance transforms and the level-set function have been exploited previously in rigid-body (Kozinska et al., 1997) and non-linear image registration (Vemuri et al., 2003), in particular to represent arbitrary shapes and their local variations (Hansen et al., 2007; Paragios et al., 2003). A recent article by Albrecht et al., which expands on previous work (Dedner et al., 2007; Lüthi et al., 2007), uses distance functions and other surface features, including curvature, to align surface renderings of human skulls and femurs (Albrecht et al., 2013). The advantage of the level-set framework is that numerical computations, such as surface curvature and normals, can be easily evaluated in the Cartesian grid without having to parameterize the surface. This implicit surface representation also prevents self-intersections and distortions during surface deformations. Topological changes, such as breaking and merging, are well defined and can be allowed or prevented (Han et al., 2002).

Multi-contrast approach

In addition to the level-set definition of the surface, additional surface or texture features can be used to drive the registration (Litke et al., 2005), such as surface curvature (Albrecht et al., 2013; Dedner et al., 2007). In our implementation, we use a total of four contrasts: a level-set representation of the cortical surface, two curvature metrics (curvedness and shape index) and, optionally, T1.

The level-set φ is modulated using the sigmoid function in Eq. (1), where the slope is steepest at the intersection with the surface. The modulated level-set $\widetilde{\varphi}$ spans the range [0, 1] within the narrow band specified by distance d. An example image is shown in Fig. 2.

$$\widetilde{\varphi}(v) = \frac{1}{1 + e^{2\varphi(v)/d}} \tag{1}$$

In addition to this contrast, which is radial to the cortical surface, we use the surface curvature to drive the registration in the tangential plane, as in Dedner et al. (2007). Our objective is to align folds that are similar in shape and size. The principal curvatures ($\kappa_{\downarrow}1$ and $\kappa_{\downarrow}2$), as well as the Gaussian and mean curvatures (K and H), both depend on the size and shape of the folds. Furthermore, they fail to distinguish certain geometries. We chose to use the following two curvature metrics: the curvedness, representing the size of the cortical folds, and the shape index, representing the local shape of the folds (Koenderink and van Doorn, 1992). These two complementary metrics are ideal for

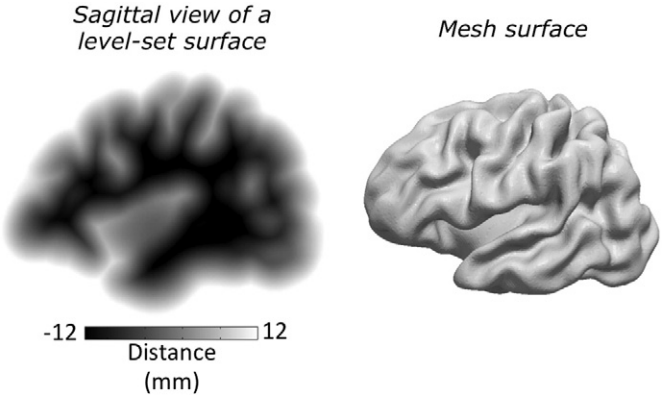

Fig. 1. Level-set representation of a cortical surface. To the left is a sagittal view of a 3D volume level-set representation of a cortical surface. The voxel values correspond to the signed distance from the cortical surface defined within a narrowband of ±12 mm. The corresponding 2D mesh representation is shown to the right.

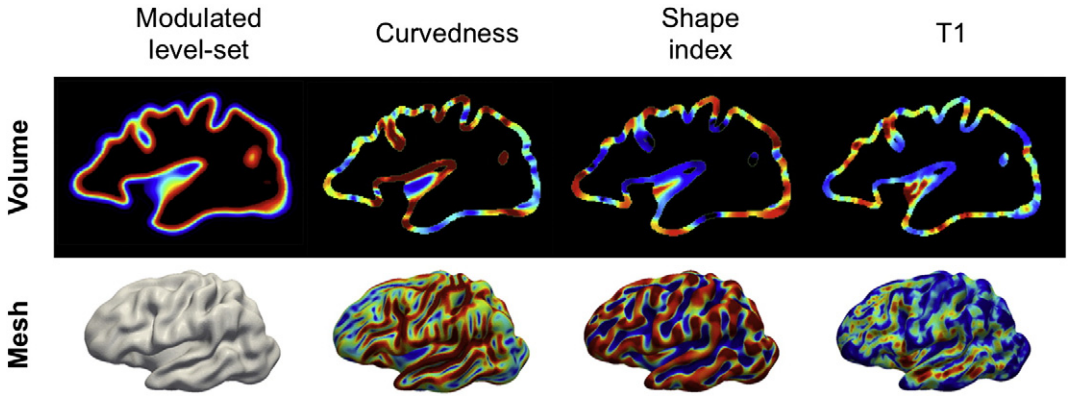

Fig. 2. Multi-modal surface-based registration image contrasts for a single inflation scale: sigmoid-modulated level-set, curvedness, shape index and T1. The volume images used for the surface-based registration are shown above the corresponding mesh representations below. Only the level-set image exhibits contrast radial to the cortical surface, all other contrasts are purely tangential to the surface.

cortical shape characterization and mapping, as shown by Tosun and Prince (2008).

The level-set is first smoothed by a 3D Gaussian kernel ($\sigma = 2$ mm). The curvedness c and shape index si of the smoothed level-set are calculated using Eqs. (2) and (3) respectively, where κ_1 and κ_2 are the two principal curvatures. An example of these two contrasts is shown in Fig. 2.

$$c = \sqrt{\frac{\kappa_1^2 + \kappa_2^2}{2}} \tag{2}$$

$$si = \frac{2}{\pi} \tan^{-1}\left(\frac{\kappa_2 + \kappa_1}{\kappa_2 - \kappa_1}\right) \tag{3}$$

Additional contrasts tangential to the cortical surface can be added to drive the surface registration. We choose to use T1 maps in order to improve the alignment of cortical areas. All tangential contrasts are linearly rescaled to the range $[-0.5, 0.5]$. Each contrast can subsequently be weighted differently for registration.

Multi-scale approach

Our multi-scale approach aligns the primary and secondary folds first, as well as the most prominent features in the other sources of contrast. The registration process consists of 20 steps, each corresponding to a different inflation scale, starting with the most inflated and leading step-by-step to the original convoluted surfaces. An affine registration is performed at the first (most inflated) scale only, where only the lobar shape of the cortex is characterized. The final registration scale has no inflation, resulting in a direct transformation between the source and target surfaces. The difference between two contiguous inflation scales is small to ensure that the transformation is smoothly defined and to minimize registration errors caused by local minima.

The level-set surface φ_0 is iteratively inflated using Eq. (4), where G is a Gaussian smoothing kernel ($\sigma = 1.5$ mm) and H is the mean curvature. The level-set surface is thus inflated by two forces: 1) a balloon force, which corresponds to the difference between the original and Gaussian smoothed level-set; and 2) a smoothing force, which corresponds to the motion under mean curvature H. The 20 inflation scales correspond to 40, 36, 32, 28, 25, 22, 19, 17, 15, 13, 11, 9, 7, 6, 5, 4, 3, 2, 1, 0 time steps (iterations) respectively, a subsample of which is illustrated in Fig. 3. The number of inflation scales and time steps per scale were chosen to ensure an accurate and smooth transformation. These parameters could be further optimized to trade-off accuracy for computational speed.

The curvature metrics are evaluated at each inflation scale; whereas the other cortical features, such as T1, are mapped to each inflation scale by coordinate tracking (Vemuri et al., 2003).

$$\frac{\partial \varphi}{\partial t} = [(\varphi - G * \varphi_0) - H] \cdot |\nabla \varphi| \tag{4}$$

The level-set narrow band in Eq. (1) is set to the maximum absolute difference between the source and target level-sets at the given inflation scale. By allowing the narrow band to shrink as the solution converges, we limit the search space of the algorithm, improving the accuracy and speed of the registration. We also take into account the maximum distance between the current and subsequent inflation scale in order to ensure a continuous multi-scale deformation that avoids local minima (Hansen et al., 2007; Paragios et al., 2003).

At each scale, our method applies SyN, a leading non-linear volume-based registration algorithm (Klein et al., 2009), to the multiple contrasts defined above. SyN is a symmetric image normalization algorithm that maximizes the cross-correlation within the space of diffeomorphic maps (Avants et al., 2008). SyN is run with the following parameters: cross-correlation metric with window radius of 3, a maximum of 100 coarse, 100 medium and 0 fine iterations, Gaussian regularization $(\sigma_{\text{similarity gradient}}, \sigma_{\text{deformation field}}) = (2, 2)$, symmetric normalization with gradient-descent step length of 0.25. All contrasts are used to

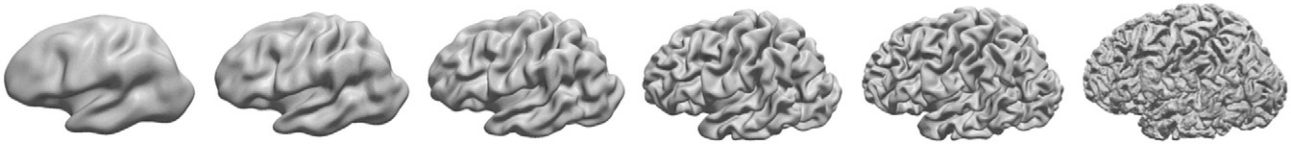

Fig. 3. Subset of surface inflation scales used for registration. From right to left, these surfaces correspond to 40, 25, 15, 7, 3 and 0 time steps of surface flow under mean curvature and Gaussian smoothing ($\sigma = 1.5$ mm).

measure convergence of the registration. An example command using all four contrasts at inflation scale 5, for instance, would be the following.

ANTS 3	*–m CC[trg_levelset_scale5.nii, src_levelset_scale5.nii, 1.0, 3]*
	–m CC[trg_curvedness_scale5.nii, src_curvedness_scale5.nii, 0.25, 3]
	–m CC[trg_shapeindex_scale5.nii, src_shapeindex_scale5.nii, 0.25, 3]
	–m CC[trg_t1_scale5.nii, src_t1_scale5.nii, 0.5, 3]
	–i 100x100x0
	–r Gauss[3,1]
	–t SyN[0.25]
	–number-of-affine-iterations 0
	–use-all-metrics-for-convergence

Group template

The procedure described above is applied to pairwise surface registration. In order to create a group atlas as an evolving template from several registration iterations, we made the following adjustments.

We calculate the group average surface mesh by applying the deformations to the target surface mesh vertices, and averaging the resulting coordinates of each source. It is often the case that the deformed target does not perfectly rest on the source surface, i.e. a residual error radial to the surface remains. This is conveniently avoided when registering 2D manifolds instead of a 3D volume. Here, this error is corrected by projecting the deformed target vertices onto the source surface using an iterative approach (Pons et al., 2006). The projection P is calculated using the source surface unit normal vector, conveniently the normalized gradient of the level-set image, and the remaining distance between the source and deformed target surfaces (i.e. the source level-set value at the deformed target coordinates).

$$P = \frac{\nabla\varphi}{|\nabla\varphi|} \cdot (-\varphi) \tag{5}$$

In areas of high curvature or complex shape, Eq. (5) may result in residual error. If the error is larger than a predefined threshold, the projection distance is halved and the procedure is reiterated from the new deformed target position. Group averages of surface features, such as curvature, T1 and cortical thickness, can also be calculated using this combination of deformation and projection.

The target atlas is typically less convoluted than the individual source surfaces, and should thus not be inflated by the same number of iterations as the source. Instead it is inflated until it matches the global shape metric of the partially inflated source surface (Tosun and Prince, 2008). This global index is the L2 norm of the mean curvature H, defined in Eq. (6) for the level set framework, i.e. the average of the mean curvature H over all voxels on the surface.

$$\|H\|_2 = \frac{1}{N}\sum_n H(n), \quad for\ n\ where\ \varphi(n) \in \left[-\sqrt{3};\sqrt{3}\right] \tag{6}$$

Software

Our novel multi-contrast surface registration algorithm has been implemented as a plug-in for MIPAV (Medical Image Processing, Analysis and Visualization) and JIST (Java Image Science Toolkit) platforms. It is part of the CBS high-resolution image processing toolbox, available on the institute's website[1] and on NITRC.[2]

[1] http://www.cbs.mpg.de/institute/software/cbs-hrt/.
[2] http://www.nitrc.org/projects/cbs-tools/.

Geometric group template

In this first experiment, we compare group templates created using MMSR, FreeSurfer (Fischl et al., 1999), the most widely used surface registration algorithm, and Spherical Demons (Yeo et al., 2010), considered the state-of-the-art technique. The alignment of the curvature metric is quantitatively compared to evaluate the precision of the registration by the three techniques.

Data acquisition and processing

Ten subjects were scanned on a 7 Tesla (T) Siemens MR scanner with a 24-channel receive-only Nova head coil. 0.7 mm isotropic T1-weighted images corrected for B1 RF transmission field inhomogeneities were acquired using the MP2RAGE (Marques et al., 2010) (TI_1/TI_2 = 900/2750 ms, TR = 5 s, TE = 2.45 ms, α_1/α_2 = 5°/3°, bandwidth = 250 Hz/px, echo spacing = 6.8 ms, partial Fourier = 6/8, GRAPPA acceleration factor 2, scan time = 11 min). An adiabatic inversion pulse was implemented to minimize sensitivity to B1 inhomogeneity (Hurley et al., 2010). Nevertheless, the image quality was impaired in the inferior temporal lobes due to insufficient B1. The latter could lead to image segmentation and surface extraction errors. Results in this area should be interpreted with caution. For future experiments, the B1 homogeneity could be improved by using dielectric pads (Teeuwisse et al., 2012).

The uniform T1-weighted images were pre-processed using the standard FreeSurfer pipeline (version 5.1.0), which resamples the data to 1 mm isotropic, and to a level-set representation within MIPAV. For MMSR, the smoothed white matter surface (*lh.smoothwm*) was converted to vtk file format using *mris_convert*. The meshes were cleaned using MeshLab[3] to remove unreferenced vertices, duplicated vertices, duplicated edges and zero area triangles, and to orient all faces coherently. The cleaned meshes were converted to a signed distance field representation within MIPAV using the method of surface pseudonormals (Bærentzen and Aanæs, 2005). MMSR is solely driven by geometrical features in this experiment (modulated level set, curvedness and shape index) for a fair comparison to FreeSurfer and Spherical Demons.

Surface registration was performed using a two-round evolving target surface. The median surface of the group was used as the initial target. The median surface was identified by taking the voxel-wise mean of the ten level-set images, and then identifying the level-set surface that is closest to this mean, i.e. with the minimal mean absolute difference between subject level-set and mean level-set. After the first round of registration, the mean surface was computed and used as the new target to which the initial surfaces were registered. The resulting group average surface, as well as the group average and standard deviation of the curvature (*lh.curv*) are compared across the three techniques.

Results

The average cortical surface of ten subjects is shown in Fig. 4 for FreeSurfer, Spherical Demons and MMSR. The mean curvature H is mapped onto the average surfaces to highlight the differences in shape between them. FreeSurfer and Spherical Demons perform very similarly. The primary folds labeled on Fig. 4 appear very clearly, including the central sulcus, the Sylvian fissure, the superior frontal sulcus, the calcarine sulcus, the parieto-occipital sulcus and the callosal sulcus. Some secondary sulci are also well aligned between subjects, including the cingulate and superior temporal sulci. The MMSR average surface is much more structured, with higher absolute curvature values, particularly in the frontal and occipital lobes. This is an indication that each individual source surface was transformed to more accurately match the target, reducing the inter-subject variability. The differences in the

[3] http://meshlab.sourceforge.net/.

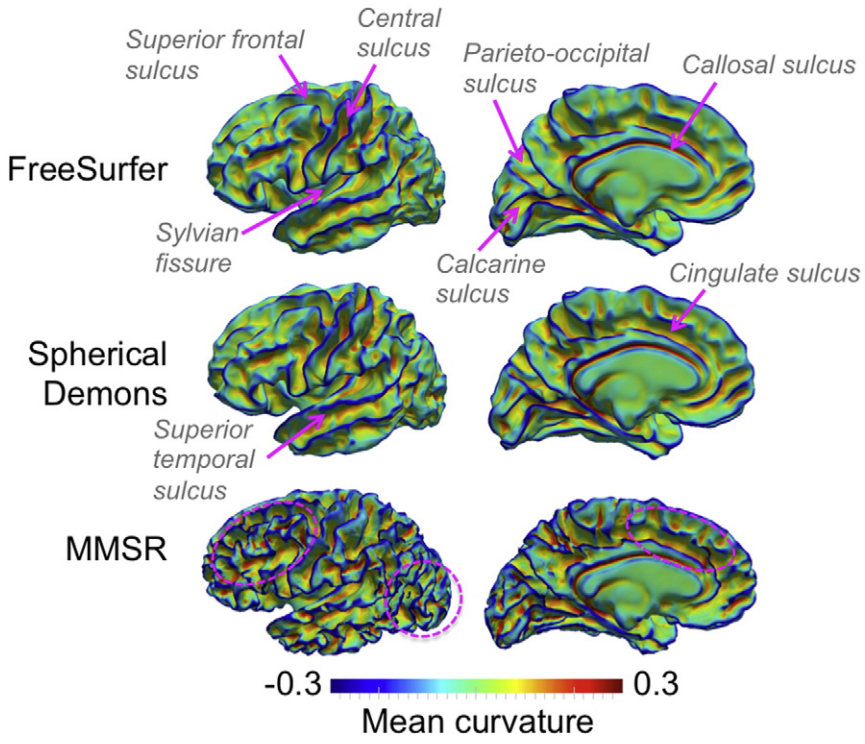

Fig. 4. Comparison of the average white matter surface of 10 subjects from FreeSurfer, Spherical Demons and MMSR. The mean curvature *H* of each respective surface is mapped onto it to help visualize their shape. The primary sulci are well aligned for the three techniques, including the central sulcus, the Sylvian fissure, the superior frontal sulcus, the calcarine sulcus, the parieto-occipital sulcus and the callosal sulcus, labeled above. Differences in shape between the three techniques in the frontal and occipital lobes are highlighted by ellipsoids. MMSR generates an average surface with much more gyrification than FreeSurfer and Spherical Demons due to a more precise alignment between the source and target surfaces.

level of smoothness of the three average surfaces is strongest in areas of tertiary folding, which exhibit stronger inter-subject variability and are thus more difficult to align.

The group average of the source surfaces' mean curvature *H* is mapped onto the average surface in Fig. 5. The mean curvature *H* is one of the metrics used by FreeSurfer (*lh.curv*) and Spherical Demons to align the surfaces, whereas MMSR uses the curvedness and shape index. Each technique results in a similar range of curvature values but with a very different structure. The individual curvature maps are better aligned in the lateral frontal cortex by MMSR, resulting in a

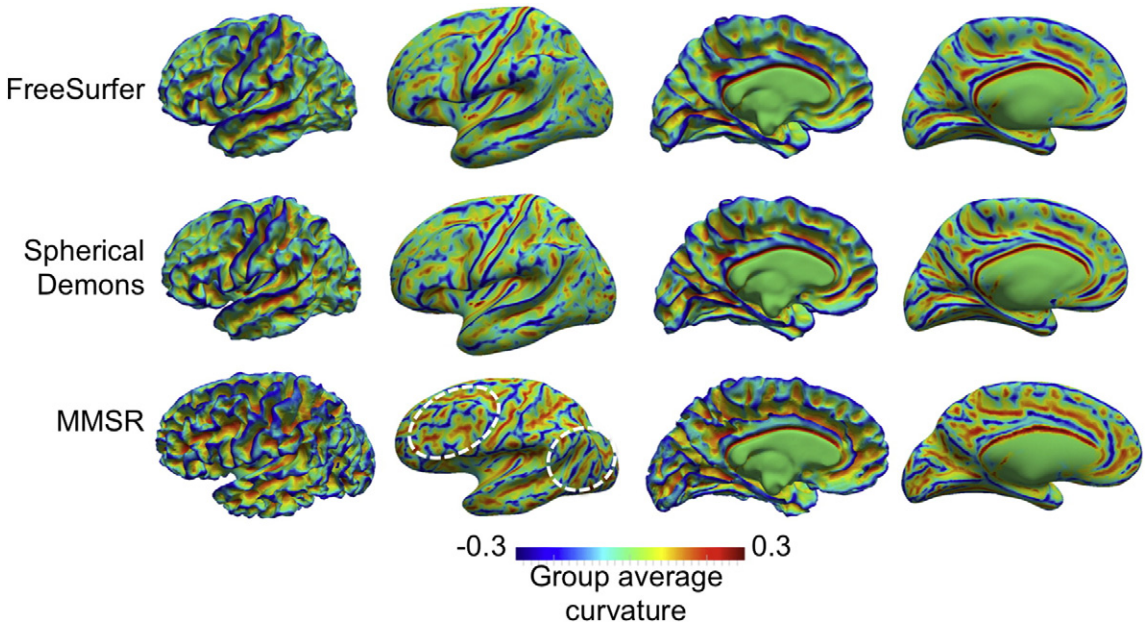

Fig. 5. Comparison of the group average of the source surfaces' mean curvature *H* mapped onto the average white matter surface for the three registration techniques. A similar range of values are represented for the three techniques, but with a very different structure. For instance, the curvature values are better aligned in the lateral frontal cortex by MMSR, as shown by the structure in the group average curvature within the white ellipsoid. There are more positive curvature values for MMSR, corresponding to sulcal fundi. This is expected for the white matter surface where the sulcal fundi are broader than the gyral crowns.

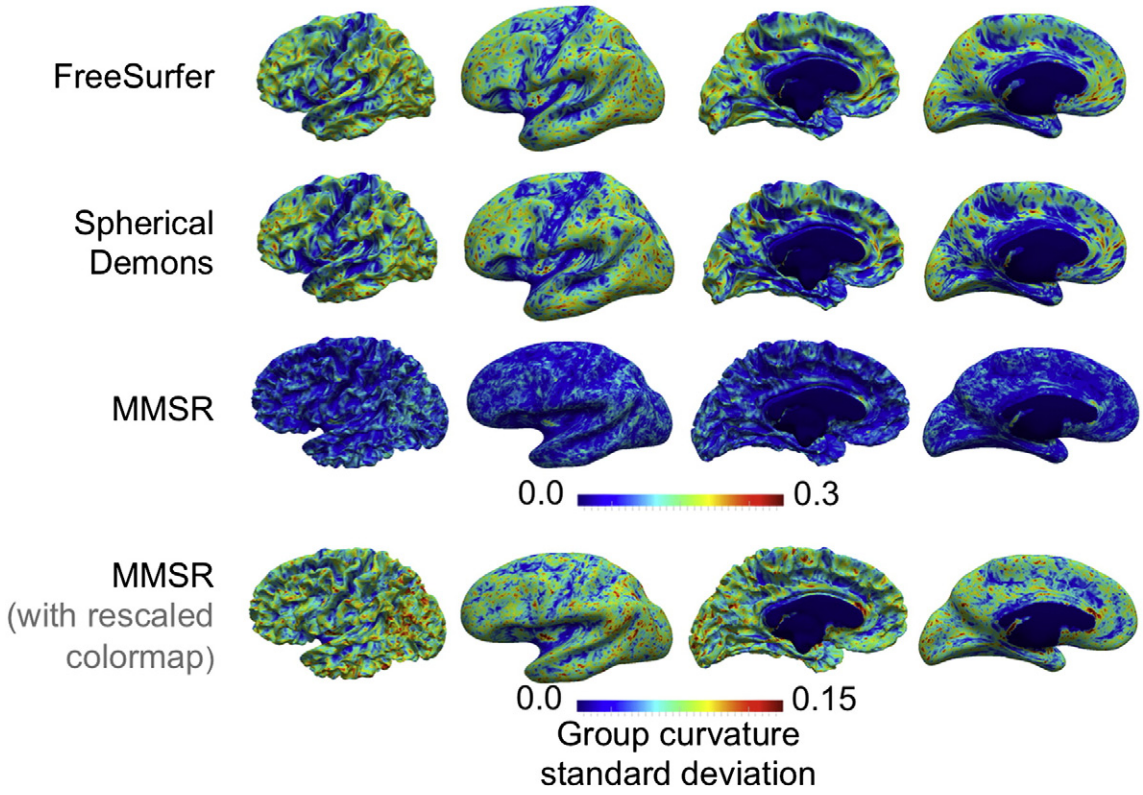

Fig. 6. Comparison of the group standard deviations in mean curvature mapped onto the average white matter surface for the three registration techniques. The standard deviations are significantly lower for MMSR. There is strong contrast between primary folds and secondary, tertiary folds for FreeSurfer and Spherical Demons, whereas MMSR performs more uniformly over the entire cortex.

more structured average curvature map. This confirms that the more complex structure of the mean surface in Fig. 4 results from a better alignment of the curvature. The MMSR average curvature map contains more positive than negative values in comparison to FreeSurfer and Spherical Demons. Since we registered the white matter surfaces, we expect this pattern as the gyral crowns are narrower than the sulcal fundi at the WM–GM tissue boundary.

The group standard deviation in mean curvature is illustrated in Fig. 6. FreeSurfer and Spherical Demons produce quite similar maps, characterized by a lower standard deviation near the primary folds, labeled in Fig. 4. Spherical Demons produces lower standard deviations than FreeSurfer in these areas. MMSR produces significantly lower standard deviations than both other methods almost everywhere. Similar to FreeSurfer and Spherical Demons, there is contrast between primary and secondary folds for MMSR, but it is much more subtle.

Our objective is to compare MMSR to FreeSurfer and Spherical Demons using their default parameters, which are applied in the majority of neuroimaging studies. A more detailed comparison over a range of regularization parameters, which affect the subsequent deformation field, is not within the scope of this paper. The combination of 1) a more gyrificated average surface, 2) a more structured average curvature and 3) significantly lower curvature standard deviation for MMSR in comparison to FreeSurfer and Spherical Demons demonstrates that MMSR achieves a more precise alignment of shape between source and target surfaces.

Alignment of manual labels

The above experiment shows that MMSR outperforms FreeSurfer and Spherical Demons at aligning the shape of the cortical surface. Since cortical folding is related to the topography of cortical areas, curvature driven surface registration is often used to indirectly align cortical areas. However, it is possible that the algorithms converge towards local minima and erroneously align mismatched cortical folds and thus differing cortical areas.

In this second experiment, we performed pair-wise registrations of a data set that has been manually labeled into different cortical areas based on cortical folding patterns. To evaluate whether MMSR is sensitive to local minima, we quantify the overlap in cortical labels between the deformed source and target surfaces. FreeSurfer is used as the benchmark in this validation.

Data acquisition and processing

We used twenty subjects from the MMRR-21 data set publicly available on Mindboggle-101 (Klein and Tourville, 2012).[4] The data set includes the cortical surfaces reconstructed using FS and manually edited cortical labels according to the Desikan–Killiany–Tourville (DKT) protocol. We chose the DKT25 cortical labeling protocol, which defines cortical regions using sulcal landmarks. This protocol combines subregions of larger gyral formations and whose divisions are not based on sulcal landmarks or are formed by sulci that are highly variable. It is thus appropriate for the evaluation of surface registration algorithms driven by cortical folding patterns.

We performed ten pair-wise registration experiments of the left hemispheres using FreeSurfer and MMSR. In FreeSurfer, pair-wise registration was performed via a template, the MMRR-21 surface template also available on Mindboggle-101. As for the previous experiment, the surface meshes were cleaned and converted to a level set representation. MMSR was solely driven by geometrical features for a fair comparison to FreeSurfer.

[4] http://mindboggle.info/.

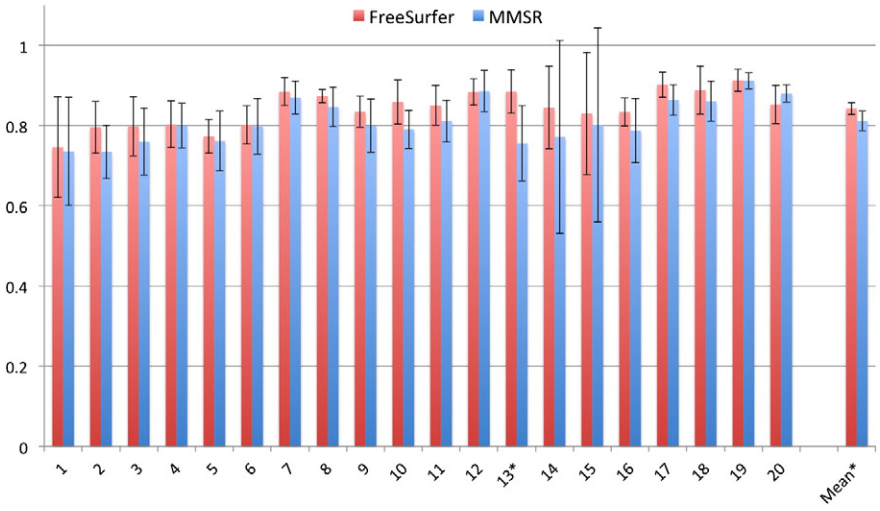

Fig. 7. Dice coefficients for each cortical label, and the mean over the whole left cortex. The * indicates structures where a statistically significant difference in alignment was measured. Overall, the performance of FreeSurfer and MMSR is very similar.

The Dice coefficients of the DKT25 labels, i.e. the overlap between the deformed source and target labels, were calculated as a measure of surface alignment. The FS surface annotations were converted into vtk files using the utilities provided by Mindboggle. The Dice coefficients were compared using a two-tailed two-sample t-test with unequal variances ($\alpha = 0.05$). The t-tests of the individual labels were corrected for multiple comparisons using the Bonferroni method.

Results

The Dice coefficients for FreeSurfer and MMSR are compared in the bar graph of Fig. 7. The corresponding cortical structures are listed in Table 1. A statistically significant difference in alignment is observed for the pericalcarine sulcus where FreeSurfer achieves a Dice coefficient of 0.88 ± 0.05, whereas MMSR achieves 0.76 ± 0.09. Otherwise, the overlap of cortical labels defined by sulcal landmarks is very similar for FreeSurfer and MMSR. The Dice coefficients averaged over all labels are slightly higher for FreeSurfer (0.84 ± 0.01) than for MMSR (0.81 ± 0.02) ($p = 0.005$ uncorrected).

Table 1
List of cortical labels from the DKT25 protocol used to quantify cortical alignment. Several of the labels were merged during the conversion from FS annotation to vtk surface.

1	Middle frontal
2	Cuneus
3	Fusiform
4	Inferior parietal
5	Inferior temporal
6	Lateral occipital
7	Lateral orbitofrontal
8	Medial orbitofrontal
9	Middle temporal
10	Parahippocampal
11	Paracentral
12	Inferior frontal: opercularis, triangularis, orbitalis
13	Pericalcarine
14	Postcentral
15	Precentral
16	Superior parietal
17	Superior temporal
18	Transverse temporal
19	Insula
20	Cingulate, precuneus, superior frontal, lingual, entorhinal, supramarginal

Few manually labeled cortical datasets are publicly available. The datasets available via Mindboggle-101 are in our opinion best-suited for surface registration validation. However, they may be biased towards FS due to the DKT cortical labeling protocol. The latter was intentionally designed to rely on region boundaries that are well suited to FreeSurfer's classification algorithm, which is based on surface registration. First, the surfaces were automatically labeled by FreeSurfer by surface registration to the DK cortical atlas (Desikan et al., 2006; Fischl, 2004). These initial labels were subsequently manually edited to ensure adherence to the DKT25 protocol. The editing procedure was guided by curvature maps, the same used to perform the registration, overlaid onto the native and inflated cortical surfaces. Due to this bias, we must be cautious in interpreting the results. This experiment should not be considered as an objective evaluation of the alignment precision, i.e. the small difference in the Dice coefficients averaged over all areas might reflect the bias in the labeling protocol rather than a more precise alignment of boundaries for FreeSurfer in comparison to MMSR. Alternatively, the precision of the alignment of cortical areas could also be evaluated using labels derived from functional MRI, as in Frost and Goebel (2012). However, the functional labels may not correspond to the cytoarchitectonic boundaries between cortical areas.

The purpose of this experiment was to evaluate the sensitivity of the techniques to local minima, which will affect the accuracy of the alignment. The small difference in the Dice coefficients between FreeSurfer and MMSR and the low standard deviations indicate that both techniques are robust to local minima. Upon detailed inspection of the individual registration results, we noticed that both FreeSurfer and MMSR grossly misaligned the pre-central (label 15) and the post-central (label 14) gyrus in one of ten subjects, resulting in the higher standard deviations. Otherwise, the differences in Dice coefficients are due to small differences in alignment at the label boundaries.

Group-wise mapping of T1 contrast

In the previous two experiments, we showed that MMSR outperforms FreeSurfer and Spherical Demons at aligning cortical surfaces based on their shape. But this improvement does not necessarily translate into improved alignment of cortical areas. As explained in the Introduction, the relationship between cortical folding and the topography of cortical areas is highly variable and has not been precisely defined. The objective of this third experiment is to demonstrate the

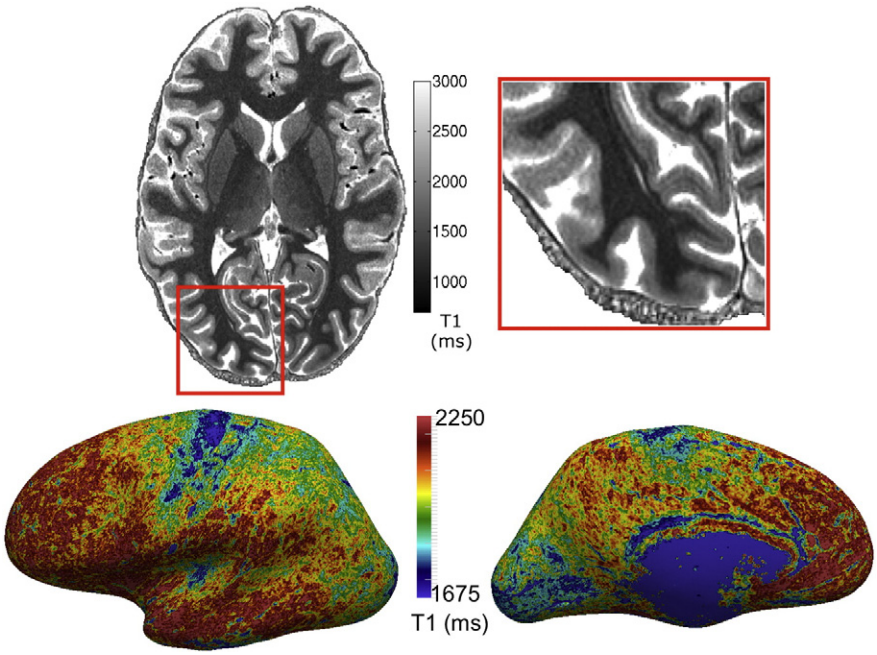

Fig. 8. 0.5 mm isotropic T1 map acquired using the MP2RAGE sequence at 7 T. The T1 map exhibits intra-cortical contrast between cortical areas and cortical layers. Top: axial view of the volume image. The stria of Gennari, for instance, is clearly visible as a band of low T1 within the primary visual cortex in the zoom-in on the right. Bottom: T1 mapped onto the inflated central cortical surface.

improvement in alignment of cortical areas achieved by introducing T1 contrast as an additional registration metric.

Data acquisition and processing

High-resolution T1 maps of ten subjects were acquired using the MP2RAGE protocol described previously. A whole brain scan was performed at 0.7 mm isotropic with a GRAPPA acceleration factor of 2 (11 min), followed by a 0.5 mm isotropic scan (28 min) of each hemisphere without acceleration, for a total scan time of 67 min. A major concern at high resolutions and of long scan times is subject motion. We selected subjects with previous scanning experience and detected no gross motion artifacts, such as ringing or blurring, in the images. An example of a $(0.5\ \text{mm})^3$ T1 map is shown in Fig. 8.

All pre-processing was performed using the CBS high-resolution toolbox. The three T1 maps were linearly co-registered into MNI space (Jenkinson et al., 2002) at 0.4 mm isotropic to minimize blurring caused by resampling, and the 0.5 mm images were fused to generate a whole brain T1 map. The resulting T1 maps were segmented (Bazin et al., 2014) and the cortical surfaces of the left hemispheres reconstructed (Han et al., 2004). The high resolution of the T1 maps results in more accurate cortical boundaries. Furthermore, the intra-cortical T1 contrast is less affected by partial volume effects with the neighboring white matter and CSF.

The cortex was divided into 20 layers, where layer 1 corresponds to the WM/GM boundary surface and layer 20 to the GM/CSF boundary surface. The 18 intermediate layers were defined using a novel volume-preserving layering model (Waehnert et al., 2014), resulting in layers that are uniformly spaced in areas of straight cortex, but non-uniformly spaced in areas of curvature in order to follow the true anatomical laminae. The level-set corresponding to the 10th layer, i.e. approximately the middle of the cortical thickness, was used for registration, as it has a fair representation of sulcal and gyral folds. Cortical profiles were reconstructed perpendicularly to the 20 layers. We averaged T1 values from the 5th to the 15th sample of the profile (approximately 25% to 75% cortical depth) to create a mean cortical T1 map that is free of partial volume effects with neighboring WM and CSF. The mean T1 map was smoothed tangentially to the surface using a Gaussian kernel ($\sigma = 2$ mm) for the purpose of registration only. To enhance registration efficiency, the level-sets and smoothed T1 maps were downsampled from 0.4 to 0.8 mm isotropic.

As for Experiment 1, surface registration was performed in two rounds using an evolving target surface. We performed three surface registration trials using MMSR. In all three trials, the radial and tangential contrasts had an equal weighting of one. The tangential contrast combinations, listed in Table 2, were: (Trial 1) curvature metrics only, (Trial 2) curvature and T1, and (Trial 3) T1 only. In Trial 2, the curvature metrics were only included during the first 10 of 20 inflation scales, such that only primary and secondary folds are used to initialize the alignment. Group averages and standard deviations of the T1 maps, level-sets, curvedness and shape index are compared across the three trials.

Table 2
Image contrast weights for the MMSR surface registration trials of Experiment 2.

	Modulated level-set	Curvedness	Shape index	T1
Trial 1	1.0	0.5	0.5	0.0
Trial 2	1.0	0.25	0.25	0.5
Trial 3	1.0	0.0	0.0	1.0

Results

The group average T1 maps, shown in Fig. 9, have a much higher contrast-to-noise ratio than the T1 maps for individual subjects, as shown in Fig. 8. In general, the group average T1 maps of the three trials are similar. This observation supports the assumption that cortical areas are correlated with cortical folding. Primary areas, such as the primary motor (M1), somatosensory (S1), auditory (A1) and visual (V1) cortices, are more densely myelinated and thus exhibit shorter T1. Several extra-striate visual areas appear as well on the occipital cortex. There is also subtle contrast in the frontal lobe corresponding to higher order cortical areas.

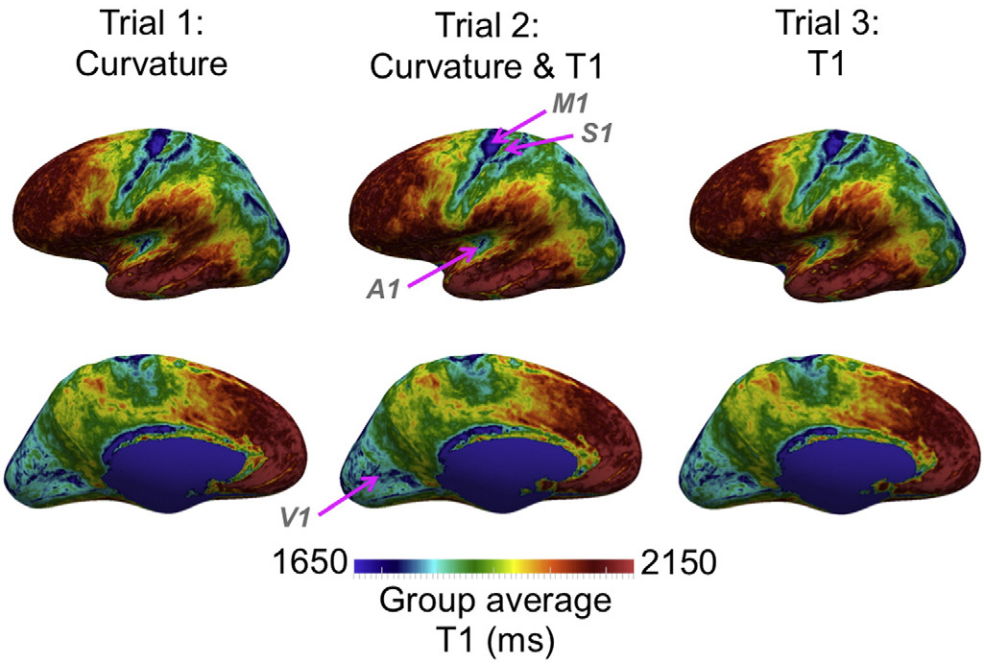

Fig. 9. Comparison of group average T1 maps created using MMSR for three different contrast combinations: curvature, curvature and T1, and T1 only. Overall, the T1 maps appear very similar. Primary cortical areas, including the primary motor, somatosensory, auditory and visual cortices, appear as clear clusters of low T1. There are however subtle improvements in alignment using T1, particularly in areas corresponding to higher order cortical areas, which are highlighted in Fig. 8.

There are small yet important differences between the group average T1 maps of the different contrast combinations, which are highlighted in Fig. 10. In the lateral view of the cortical surface, we can clearly see the boundaries of areas M1, S1 and A1 for all three trials, particularly on the inflated surfaces. There is a small improvement in alignment perpendicular to the main cortical folds when including T1, mainly along the frontal boundary of M1 and posterior boundary of S1. Cortical curvature only aligns the cortex in the direction perpendicular to the cortical folds, whereas T1 can also improve the alignment in the direction parallel to the folds. For example, with the T1 contrast we see an improvement parallel to the Sylvian fissure for A1, resulting in a more distinct structure with sharper boundaries, and parallel to the precentral gyrus for M1. More interestingly, we can see improvements in the alignment of non-primary cortical areas. The motion sensitive visual complex MT+ on the lateral occipital cortex is an area characterized by high inter-subject variability in cortical folding. The inclusion of T1 contrast tightens the MT+ cluster and sharpens its boundaries with neighboring areas, mainly posterior to MT+. The inclusion of T1 contrast also sharpens the boundaries of other extra-striate visual areas, including the ventral intra-parietal area VIP. The alignment of the frontal cingulate cortex, which has distinct T1 contrast as well, is shown in the medial view in Fig. 10. Although the T1 contrast in the frontal lobe is more subtle, it still improves the alignment of cortical areas in comparison to using cortical curvature only. In the frontal lateral view in Fig. 10, we can see sharper, more structured boundaries in the group T1 map for Trials 2 and 3, including a cluster of low T1 corresponding to the frontal eye field (FEF), and a second less pronounced cluster putatively corresponding to Broca's area.

The above differences in the alignment of T1 are also reflected in the group T1 standard deviation, shown in Fig. 11. The T1 standard

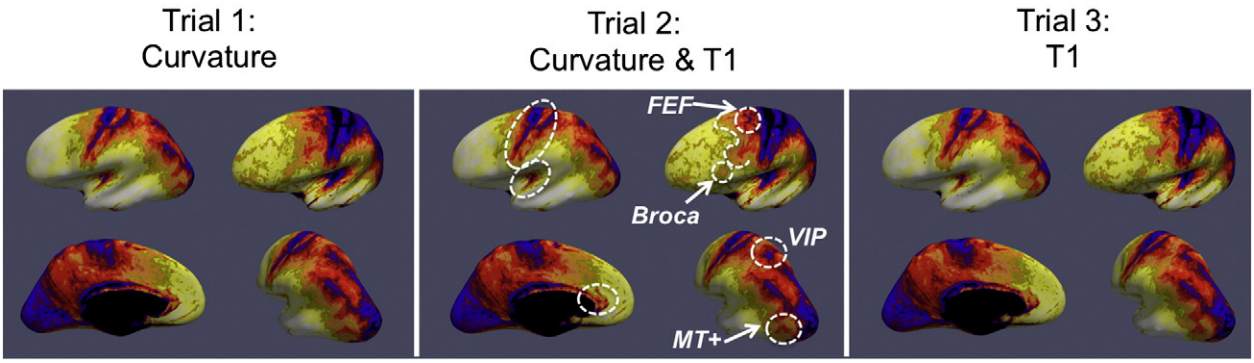

Fig. 10. Multiple views of the group average T1 maps created using three different contrast combinations. The colormaps are adjusted for each different view point to enhance the local contrast between cortical areas. Differences between the contrast combinations are highlighted using white ellipsoids. In the lateral view (top left), we can see differences for the primary motor M1, somatosensory S1 and auditory A1 cortices mainly in the direction parallel to the main cortical fold. In the lateral-frontal view (top right), the T1 map frontal to M1 has a more distinct structure for Trials 2 and 3. There is also a cluster of decreased T1 corresponding to the frontal eye field FEF, and a more subtle inferior cluster putatively corresponding to Broca's area. In the medial view (bottom left), the frontal callosal and cingulate cortex are better aligned. In the occipital-lateral view (bottom right), the motion sensitive visual complex MT+ and ventral intra-parietal area VIP are also better aligned.

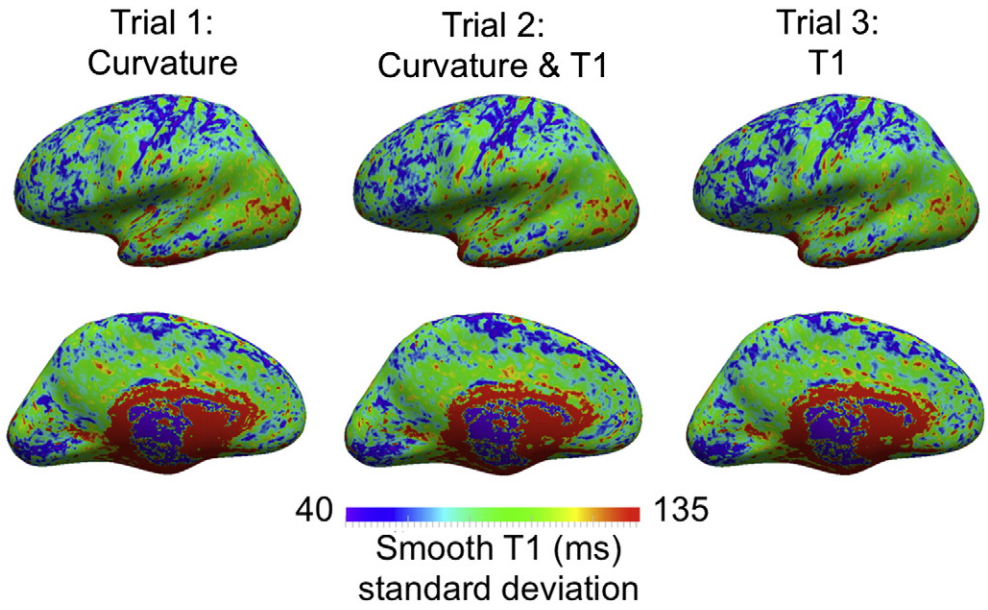

Fig. 11. Comparison of the group standard deviation in T1 created using MMSR for three different contrast combinations. The standard deviation decreases for Trials 2 and 3 in the same areas where we highlighted differences in the average T1 maps in Figs. 7 and 8.

deviation decreases when T1 contrast is used to drive the registration, in Trials 2 and 3. The decreases coincide with the areas of improved T1 alignment described above.

The addition of T1 maps to drive the surface registration has an impact on the shape of the average surface and the alignment of the geometric features, including the level-set and curvature metrics. The

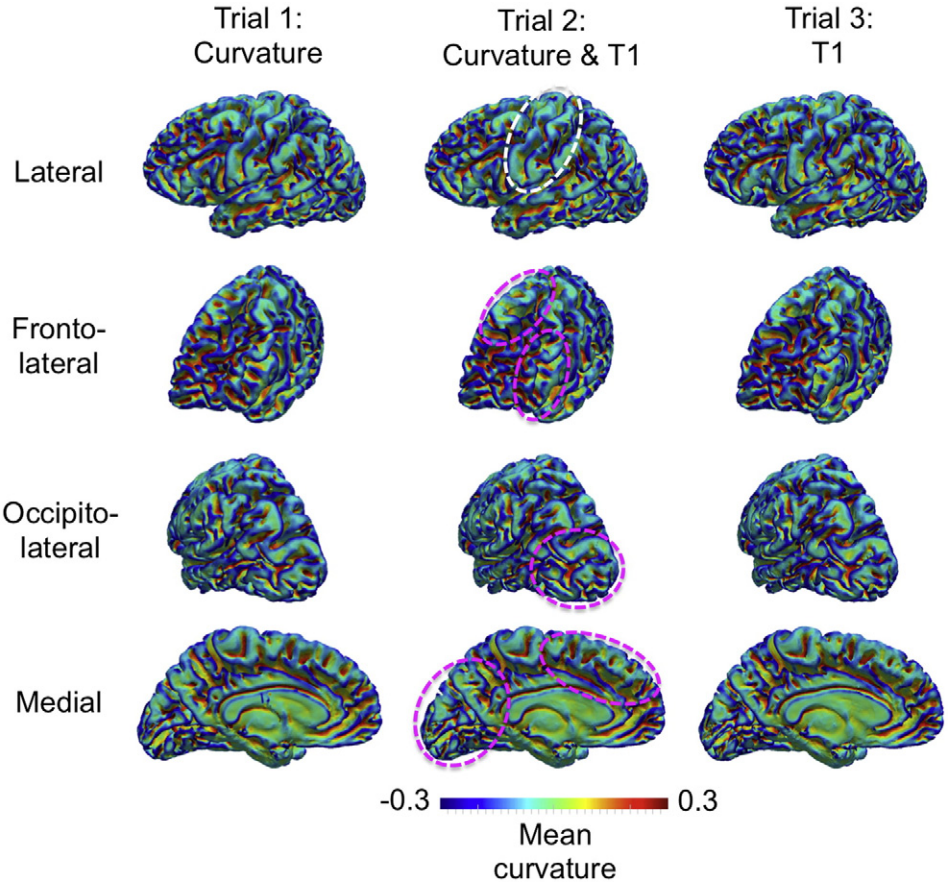

Fig. 12. Comparison of the average central cortical surface across 10 subjects using MMSR for three different contrast combinations. The mean curvature is mapped onto the surfaces to help visualize their shape. The primary cortical folds are well aligned for all three trials, as shown by the similarity around the central sulcus (white ellipsoid). We can see some differences in areas of higher gyrification and inter-subject variability, highlighted by the magenta ellipsoids in the frontal and occipital cortex. Overall, the magnitude of the curvature values is highest for Trial 1, which only includes geometry metrics.

group average surfaces for the three trials are shown in Fig. 12, mapped with their respective mean curvature. The shape of these surfaces is very similar near primary folds, such as the central sulcus. The differences in surface shape between the three trials occur in areas of high inter-subject folding variability. Trial 1 results in the average surface with the most pronounced folding; however, a more gyrificated average surface does not equate to a better alignment of cortical areas in this experiment. The smoother regions in Trials 2 and 3 can result from improved alignment of T1 contrast in areas where cortical areal boundaries have a weak relationship with cortical folding patterns. On the other hand, a smoother surface can also result in an area of poor T1 contrast where the method lacks information to properly align the surfaces. Trial 2 presents a compromise where curvature metrics are used to initialize the registration of primary and secondary folds, but the fine registration is based on T1.

The group standard deviations of the three geometry metrics are shown in Fig. 13. The level-set standard deviation represents the remaining radial distance between the registered surfaces. These values are lowest for Trial 1, which uses only geometry metrics to align the surfaces. For the subsequent trials, the contrast between primary folds and the rest of the cortex is stronger. Similar to the level-set, there is a tradeoff between the alignment of curvature metrics and the alignment of T1.

The T1-based registration results depend on the quality of the T1 maps, including resolution and contrast-to-noise, and the accuracy of the cortical surface extraction. Errors in the definition of cortical boundaries, or insufficient resolution, will result in sampling the T1 in the WM or CSF. The T1 contrast between tissues is higher than the intra-cortical T1 contrast. It is thus important to inspect the T1 times sampled at the cortical surface prior to registration.

As discussed by Waehnert et al. (2014), the T1 times sampled within the cortex correlate with cortical curvature. This is partly due to partial volume effects as well as the varying thickness of the cortical laminae (Bok, 1929). Lutti et al. (2014a) perform a linear regression of T1 against curvature and cortical thickness to remove this effect. Shafee et al. (2014) recently showed the impact of partial volume correction on surface myelin maps. In our opinion, the best approach would be to image the cortex at a higher resolution (<0.8 mm isotropic) to minimize partial volume effects, and to use the equi-volume layering approach (Waehnert et al., 2014) applied here, which respects the natural coordinate system of the cortex in areas of curvature. These pre-processing details are important as the T1 contrast between cortical areas may be

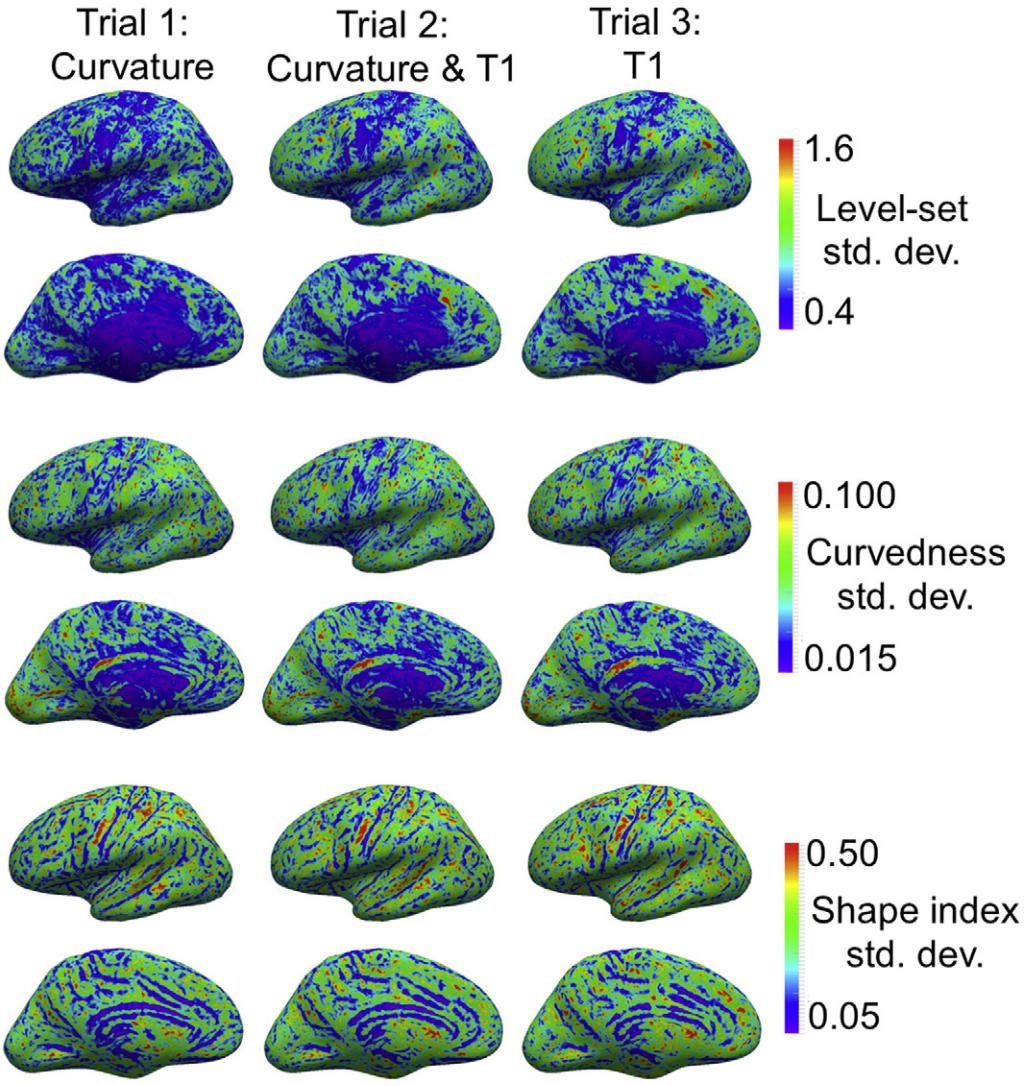

Fig. 13. Comparison of the group standard deviations in geometry metrics created using MMSR for three different contrast combinations. The metrics include, from top to bottom, the level-set, curvedness and shape index. All standard deviations are lower for Trial 1, which excludes T1 contrast. The areas that are better aligned in Fig. 8 and have a lower T1 standard deviation in Fig. 9, tend to also have a higher standard deviation in the geometric metrics. There is thus a trade-off between the alignment of cortical areas as defined by T1, and the shape of the cortex.

smaller or comparable to the T1 contrast between cortical layers. Otherwise, the registration results will be similar to a shape based alignment.

Application: high-resolution group T1 map at multiple cortical depths

Data processing

To highlight the potential impact of MMSR on the future of in vivo brain mapping, we applied the transformations from Trial 3 above to $(0.5\ mm)^3$ T1 maps sampled at four cortical depths. Excluding the first and last pairs of computed intra-cortical layers to minimize partial volume effects with WM and CSF, we divided the remaining 16 of the 20 layers into 4 groups: Layer 1 (deep — near white matter surface), Layer 2 (inner middle), Layer 3 (outer middle), and Layer 4 (outer — near pial surface).

Results

The resulting high-resolution group average T1 map of the cerebral cortex is shown in Fig. 14. This is a 3D T1 map of the cortex within its natural coordinate system, and reflects its myeloarchitecture. In general, T1 decreases with cortical depth, as shown in the first two rows of Fig. 14. In the bottom two rows, the T1 color-map is optimized for each cortical depth to illustrate that the intra-cortical contrast varies both tangentially and radially to the surface. The contrast at areal boundaries is thus depth dependent. The most striking example is the greater contrast between M1 and S1 in Layer 4 in comparison to deeper Layer 1.

Myelin maps of the cortex have previously been sampled at multiple cortical depths, but at a much lower resolution. R1 (1/T1) maps at $(0.8\ mm)^3$ were shown at three cortical depths (0.8, 0.5 and 0.2 depth fraction) (Lutti et al., 2014b) and T1-weighted/T2-weighted images at $(1.2\ mm)^3$ were shown at two cortical depths (Shafee et al., 2014). Here, we present a much higher resolution quantitative myelin map. Due to the equi-volume layering approach, the four layers in Fig. 14 follow the true anatomical laminae in areas of curvature. By minimizing partial volume and curvature biases, the tangential and radial myeloarchitecture of the cortex is more clearly visualized.

Discussion

Comparison to leading surface registration techniques

We developed a novel surface registration technique, MMSR, which provides a high-resolution direct symmetric diffeomorphic transformation between two surfaces. We compared MMSR to two of the leading surface registration techniques: FreeSurfer and Spherical Demons. MMSR creates more detailed group average surfaces, more structured group average curvature, and lower group curvature standard deviation. These three results clearly point to MMSR's superior precision in the alignment of cortical shape. MMSR's alignment accuracy, and susceptibility to local minima, were evaluated using manual cortical labels based on sulcal landmarks. MMSR's performance was comparable to FreeSurfer, the benchmark for this validation dataset. There are several differences between the implementations of the three registration techniques, mainly the coordinate system, multi-scale approach and geometric features, which are discussed below.

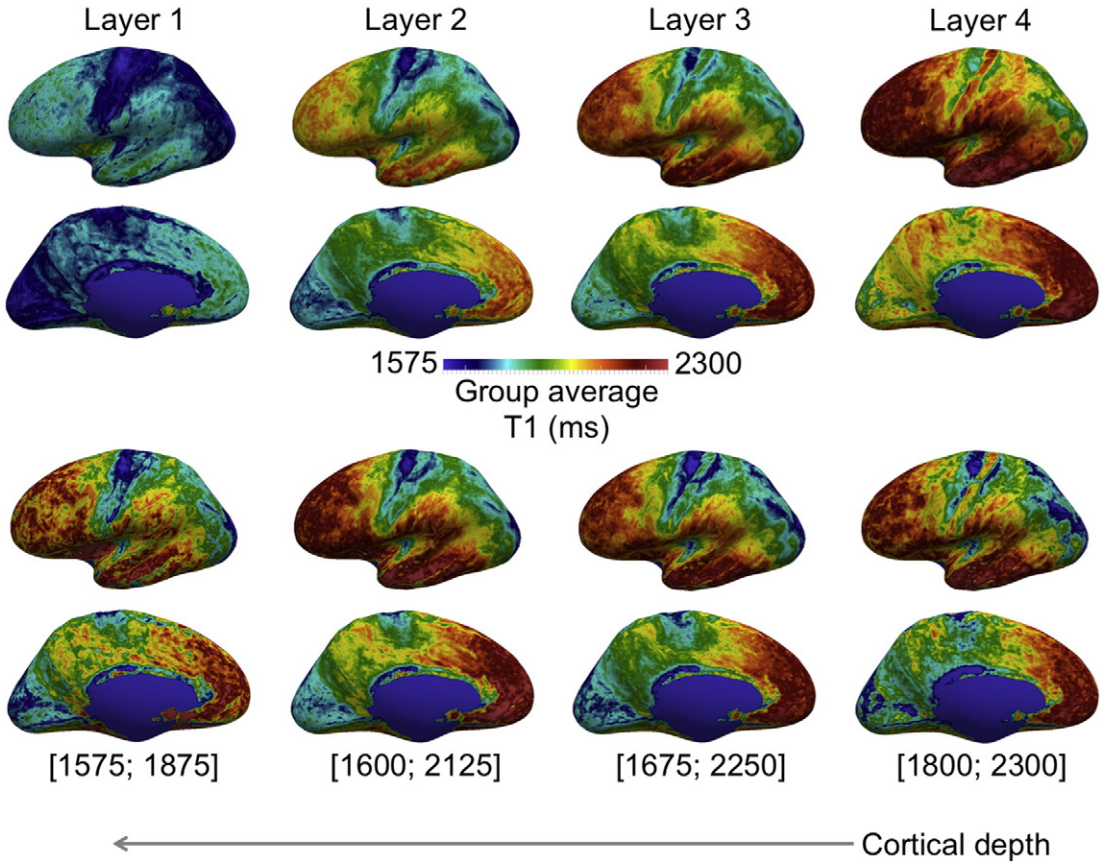

Fig. 14. Group average (N = 10) $(0.5\ mm)^3$ T1 map at four cortical depths. The T1 maps were registered using MMSR with T1 contrast only. The T1 maps in the first two rows are represented using the same colormap, highlighting the T1 gradient with cortical depth. The colormaps of the T1 maps in the bottom two rows have been adjusted for optimal contrast at each depth individually. The contrast between cortical areas varies with cortical depth, and reflects myeloarchitectonic descriptions of the cortex.

In order to align 2D cortical surfaces, the latter are first typically unfolded to a manifold with a standard coordinate system, such as a plane or, most often, a sphere. Both FreeSurfer and Spherical Demons work within a spherical framework, which has several advantages. Firstly, the topology of the cerebral cortex is preserved during the mapping to a spherical representation. Secondly, the spherical coordinate system is computationally attractive as it facilitates the calculation of metric properties, such as geodesic distance, area and angle. The correspondence across two cortical surfaces is established by warping of their spherical coordinate systems, the surfaces are not actually deformed in 3D space during the alignment process. The resulting mapping is between vertices, which have coordinates in the original 3D Cartesian space. Unfortunately, spherical reparameterization induces metric distortions that can affect the quality of the subsequent alignment. There are two different methods for unfolding the cortex to a sphere: iteratively deforming the vertices of a mesh until it is convex and then projecting it to a sphere, or conformal mapping. The former method, implemented in FreeSurfer, is computationally intensive, and the latter is very sensitive to details in the mesh representation. In both cases, there is no guarantee that two cortical surfaces will end up close on the sphere. An alternative is to work with partially inflated surfaces, which simplify the shape correspondence between subjects while reducing the metric distortions with respect to spherical mapping (Eckstein et al., 2007; Tosun and Prince, 2008). In contrast, we work here in the original 3D space. We employ partially inflated surfaces as the methods above in order to initialize the shape correspondence, which is then refined to align less and less inflated versions of the surface. The final transformation is performed between the original, non-inflated, surfaces; thus the accuracy and precision of the final transformation is not hindered by geometric distortions caused by reparameterization.

A variety of cortical geometry features can be used to drive surface registration: manually or automatically defined landmarks such as sulcal curves (Joshi et al., 2010; Perrot et al., 2011; Van Essen, 2005), automatic shape features such as curvature and sulcal depth (Fischl et al., 1999; Goebel et al., 2006; Tosun and Prince, 2008; Yeo et al., 2010), or a combination of both (Du et al., 2011; Park et al., 2012; Zhong et al., 2010). A comparison of the leading techniques is presented by Pantazis et al. (2010). Landmark-based registration has the advantage of being flexible as one can make the most of neuroanatomical expertise and choose the landmarks that drive the registration. The registration will be most accurate near these features, and is smoothly extended between them. Alternatively, cortical features derived at each vertex, such as curvature, can be aligned. Feature-based registration has the advantage of being fully automated, although the results vary depending on the feature used. Multi-scale registration can be performed by using features that represent different scales of cortical folding. Both FreeSurfer and Spherical Demons use sulcal depth, which highlights the primary and secondary folds, and mean curvature, which also characterizes tertiary folds (Fischl et al., 1999; Yeo et al., 2010). The features can also be smoothed by varying amounts along the surface (Goebel et al., 2006), or evaluated at different surface inflation scales before being mapped onto the sphere (Tosun and Prince, 2008). In our implementation, similar to the latter by Tosun and Prince, we evaluate the surface curvedness and shape index at each inflation scale.

The advantage of using these two curvature metrics is that they can easily and efficiently be calculated in the Cartesian grid of the level-set framework at each inflation scale. Calculating sulcal depth, on the other hand, is less straightforward. It first requires the definition of a convex hull from which the Euclidean or geodesic distance (shortest path along the surface) (Rettmann et al., 2002), for instance, can be calculated. The inclusion of sulcal depth may improve sulcal alignment and will be considered in future applications of MMSR. However, a detailed evaluation of the different curvature metrics and their impact on alignment using MMSR is not within the scope of this paper.

An inverse mapping between two surfaces that preserves the topology is often desired. This causes many surface registration algorithms to be computationally expensive. In FreeSurfer, soft regularization constraints are implemented to encourage invertibility. An alternative is to work within the group of diffeomorphisms, which is slow and memory demanding. Spherical Demons applies the Diffeomorphic Demons algorithm to the sphere to achieve invertibility, but the transformation path is not a geodesic within the group of diffeomorphisms. Morphometry studies based on the analysis of the deformation field can thus not be performed. MMSR uses the SyN algorithm, which outputs a symmetric diffeomorphic transformation. The resulting transformation path is geodesic between the surfaces within the native 3D space.

We developed this novel surface registration framework with flexibility in mind. Firstly, the level-set framework is very convenient as all the processing is performed in Cartesian space. Any volume image, such as functional MRI results, can easily be sampled at the surface. Unlike most techniques, our level-set framework is not limited to a spherical topology; on the contrary, it can be generalized to surfaces with any topology. In addition, multiple surfaces can be defined using multiple level-sets within the same volume image (Bogovic et al., 2013). This could be very useful for whole brain registration where the cortex and subcortical structures are represented as surface level sets and deformed simultaneously. This would result in a single coordinate system for the whole brain. Other combined volume and surface registration techniques have been proposed. Postelnicu et al. first align the cortical surfaces using the spherical representation. The result is a 1 to 1 mapping between the surfaces in Euclidean space. The transformation is subsequently diffused to the rest of the brain volume, and finally refined for subcortical structures using intensity based volume registration (Postelnicu et al., 2009). Joshi et al. reparameterize the brain volume to a unit ball. Image intensity and cortical features are used to find a surface and volume alignment (Joshi et al., 2009). The advanced volume-based method HAMMER (hierarchical attribute matching mechanism for image registration) (Shen and Davatzikos, 2002) incorporates geometric features of the cortex to perform a simultaneous whole brain alignment. But the mapping accuracy of the cortex is lower than that for surface based approaches. Large deformation diffeomorphic metric mapping (LDDMM) methods have also been developed for whole brain alignment based on intensity (Beg et al., 2005) and the combination of gyral/sulcal curves, cortical surface, and intensity image volume in a unified manner (Du et al., 2011).

We performed surface registration experiments on 1 mm and 0.8 mm isotropic level-set surfaces in this manuscript. MMSR has been applied to data up to 0.4 mm isotropic. The minimal resolution is that required to accurately model the cortical surface using a level-set representation. Typically, a resolution of 1 mm is used, but there are advantages to higher resolution representations (Lutti et al., 2014a). The chosen resolution will also depend on the resolution of the additional contrasts, such as curvature, T1 or functional data, used to align the surfaces.

The differences in implementation discussed above collectively result in an accurate and more precise registration of cortical surfaces using MMSR. The improved registration precision of MMSR could have a significant impact on cortical morphometry studies. MMSR better aligns common geometric features in a group of surfaces, resulting in more detailed group atlases of cortical geometry. Consequently, the sensitivity of our technique to subtle differences in cortical morphology may also be enhanced.

Improving the alignment of cortical areas using T1

The main motivation for developing this novel surface registration technique was to improve the alignment of cortical areas using microstructural MR contrast. We applied our multi-contrast registration technique to T1 maps and achieved an improvement in the alignment of these myelin maps.

Overall, the group average surfaces and group average T1 maps were quite similar whether curvature metrics and/or T1 maps were used to drive the registration. This observation is in agreement with previous studies that show that the position of cortical areas can be predicted to a certain extent by the cortical folding patterns. These same studies discuss the limitations of this relationship, which is weakened for higher order cortical areas. The results from Group-wise mapping of T1 contrast section show improvements in the alignment of cortical areas using T1 contrast. There is however a trade-off between the accuracy of surface alignment with respect to folding and T1. The choice of registration metric depends on the objective of the study. For the alignment and interpretation of functional data, for instance, T1 would be more suitable.

Recently, Robinson et al. also showed an improved alignment of cortical areas using surface-based registration of myelin-based MR contrast (Robinson et al., 2014). They introduced a Multi-modal Surface Matching (MSM) algorithm that is similar in accuracy to FreeSurfer and Spherical Demons, and produced a group average T1-weighted/T2-weighted image with sharper contrast in some areas in comparison to FreeSurfer and Spherical Demons. Their group average is however not as sharp, nor as detailed, as the group average T1 map in Fig. 14. This could be due to differences in the surface registration technique and in the quality of the "myelin maps" used. In their case, the surface myelin maps are derived from 3 T MRI data of lower spatial resolution (0.7 mm isotropic) from the Human Connectome Project, and projected onto a mesh containing ~140,000 vertices per hemisphere with vertex spacings of ~1 mm. In contrast, we acquired 0.5 mm isotropic T1 maps, corresponding to a 2.744-fold reduction in voxel volume. The images were processed in 0.4 mm isotropic space, corresponding to a mesh of ~850 000 vertices per hemisphere. Our higher-resolution and equi-volume layering approach both reduce the effect of cortical curvature on the surface T1 maps, and thus on the resulting alignment.

Although several MR contrasts are correlated with myelin density, T1 maps have the advantage of being quantitative. This minimizes the spatial bias caused by B1 inhomogeneity, for instance, and reduces the intra- and inter-subject variability. T1 has been shown to be mainly correlated with myelin content, whereas T2* is correlated with both myelin and iron (Stüber et al., 2014), which are assumed to be co-localized in the cortex. Other quantitative image contrasts that reflect myelin content exist, such as magnetization transfer and myelin water imaging, but these have an intrinsically lower signal to noise ratio, and are currently limited in resolution, even at 7 T.

Myelin-based contrast has the anatomical disadvantage of being non-uniform across the cortex: the contrast between cortical areas in the frontal lobe is much lower than the contrast between cortical areas in the occipital lobe, due to the well-known decreased cortical myelin density in these regions (Glasser et al., 2014; Hopf, 1955, 1956, 1957). In addition, the dynamic range of T1 values over the whole cortex is much larger than the local T1 contrast between neighboring cortical areas. In areas where there is lower contrast, the alignment of cortical areas will be decreased. The alignment of cortical areas that exhibit strong T1 contrast may however also improve the alignment of the neighboring ones, assuming that the topology of cortical areas is consistent across subjects. It is our view that cortical curvature should not be used in addition to T1, as this would include a spatially varying bias in the resulting transformation. Accordingly, in Trial 2, we used the curvature metrics to initialize the alignment only by including it in the first 10 of 20 surface inflation scales. In future works, T1 contrast could be enhanced by spatially weighting the T1 map and using depth-dependent contrast.

The application of surface based registration to cytoarchitectonic data revealed a stronger relationship between cortical folding and cortical boundaries than originally anticipated from non-linear volume registration (Fischl et al., 2008). The study by Fischl et al. concluded, however, that the relationship was variable across the cortex, weaker in higher order cortical areas. These areas also happen to exhibit more variable folding patterns that are more difficult to align across individuals, as shown by the smooth frontal lobe of the average surface produced by FreeSurfer and Spherical Demons in Fig. 4. The variability in folding patterns and relative position of cortical boundaries both stem from later development in comparison to primary cortical areas. It is possible, however, that the relationship between cortical folding and cortical boundaries is stronger than currently estimated in these areas. Studies to date may have been limited by the accuracy of the surface registration techniques used. In this article, we present a more precise registration of cortical folds. MMSR could therefore be used to more accurately evaluate the relationship between cortical folding and cortical boundaries.

Applications to brain mapping

The exceptional image quality of the T1 maps in combination with our novel T1-based surface registration algorithm allowed us to present a group average high-resolution T1 map with unprecedented structural detail at the group level, including laminar contrast, that agree with myeloarchitectonic descriptions of the cortex. Such a high-resolution in-vivo myeloarchitectonic atlas of the whole cortex can be used to more accurately delineate cortical areas in the atlas, and in individual subjects via T1-based surface registration to the atlas. This contribution represents a significant step towards the ultimate goal of in-vivo brain mapping based on microstructure in individuals, and the much-needed attribution of functional activity to its specific neuroanatomical substrate (Turner, 2013, 2014). It would be very interesting to compare our MR-based in vivo myelin maps to the myeloarchitectonic atlas recently presented by Nieuwenhuys et al. (2014), which is expected to be released soon as a 3D atlas in MNI space.

Our method can be extended to other MR contrasts of tissue microstructure, such as T2* and quantitative susceptibility mapping (QSM) which both show intra-cortical contrast that depends on iron content. These additional sources of contrast may help align cortical features that are less clear in T1 maps. Multi-contrast surface-based atlases could be used to investigate the relationship between myelin and iron content throughout the cortex. Although it is preferable to use quantitative images that are more biologically specific, bias free and reproducible, MMSR could also be applied to T1-weighted images, T1/T2-weighted images or any other image that shows intra-cortical microstructural contrast.

Recent articles propose to use contrasts that are complementary to microstructure, such as functional or connectivity data, to improve surface-based registration of cortical areas. Sabuncu et al. improve the alignment of functional neuroanatomy by using spatial patterns of fMRI-based neural activity, elicited by viewing a movie (Sabuncu et al., 2010). Frost and Goebel use regions-of-interest derived from task-based fMRI to improve local alignment (Frost and Goebel, 2013). Functional connectivity inferred from resting-state fMRI (Robinson et al., 2014) and anatomical connectivity inferred from diffusion-weighted MRI and tractography (Petrović et al., 2009) have also been used to drive surface registration.

Our multi-modal method can use any image contrast to drive the registration in addition to or instead of curvature and/or T1. Future applications of MMSR could include the alignment of large multi-modal data sets, such as the Human Connectome Project (Van Essen et al., 2012). This is a complex task as the relationship between structure, function and connectivity may not be consistent across subjects, and are expected to change under various pathological conditions.

Conclusion

High-resolution and quantitative data sets are becoming more widely available with developments in image acquisition at 3 T and higher field strengths. These data bring new challenges and opportunities to

image processing. High-resolution T1 maps acquired at 7 T show intracortical contrast that reflects the myeloarchitecture of the cortex. The motivation for this work was to improve the alignment of cortical areas using T1 maps. We presented a novel multi-contrast multi-scale surface registration (MMSR) framework that provides a direct symmetric diffeomorphic transformation between surfaces. MMSR generates a more precise alignment than the leading surface registration algorithms. We demonstrated that the inclusion of T1 maps improves the alignment of cortical areas. Finally, we present a high-resolution group average 3D T1 map of the cerebral cortex, with unprecedented detail. Due to its flexible level set framework, precision in cortical alignment and multi-modal approach, MMSR could have a significant impact on a wide range of neuroimaging studies, including cortical morphometry, parcellation, and structure-function studies.

References

Albrecht, T., Dedner, A., Lüthi, M., Vetter, T., 2013. Finite element surface registration incorporating curvature, volume preservation, and statistical model information. Comput. Math. Methods Med. 1–14.

Amunts, K., Malikovic, A., Mohlberg, H., Schormann, T., Zilles, K., 2000. Brodmann's areas 17 and 18 brought into stereotaxic space — where and how variable? Neuroimage 11, 66–84.

Amunts, K., Schleicher, A., Zilles, K., 2007. Cytoarchitecture of the cerebral cortex — more than localization. Neuroimage 37, 1061–1068.

Avants, B.B., Epstein, C.L., Grossman, M., Gee, J.C., 2008. Symmetric diffeomorphic image registration with cross-correlation: evaluating automated labeling of elderly and neurodegenerative brain. Med. Image Anal. 12, 26–41.

Bærentzen, J.A., Aanæs, H., 2005. Signed distance computation using the angle weighted pseudonormal. IEEE Trans. Vis. Comput. Graph. 11, 243–253.

Bazin, P.-L., Weiss, M., Dinse, J., Schäfer, A., Trampel, R., Turner, R., 2014. A computational framework for ultra-high resolution cortical segmentation at 7 Tesla. Neuroimage 93, 201–209.

Beg, M.F., Miller, M.I., Trouvé, A., Younes, L., 2005. Computing large deformation metric mappings via geodesic flows of diffeomorphisms. Int. J. Comput. Vis. 61, 139–157.

Bogovic, J.A., Prince, J.L., Bazin, P.-L., 2013. A multiple object geometric deformable model for image segmentation. Comput. Vis. Image Underst. 117, 145–157.

Bok, S.T., 1929. Der Einfluss der in den Furchen und Windungen auftretenden Krümmungen der Grosshirnrinde auf die Rindenarchitektur. Z. Neurol. Psychiatry 121, 682–750.

Bridge, H., Clare, S., Jenkinson, M., Jezzard, P., Parker, A.J., Matthews, P.M., 2005. Independent anatomical and functional measures of the V1/V2 boundary in human visual cortex. J. Vis. 5, 93–102.

Brodmann, K., 1909. Vergleichende Lokalisationslehre der Großhirnrinde in ihren Prinzipien dargestellt auf Grund des Zellenbaues.

Cohen-Adad, J., Polimeni, J.R., Helmer, K.G., Benner, T., McNab, J.A., Wald, L.L., Rosen, B.R., Mainero, C., 2012. $T(2)^*$ mapping and B(0) orientation-dependence at 7 T reveal cyto- and myeloarchitecture organization of the human cortex. Neuroimage 1–9.

Dedner, A., Marcel, L., Albrecht, T., Vetter, T., 2007. Curvature guided level set registration using adaptive finite elements. Lect. Notes Comput. Sci. Pattern Recogn. 4713, 527–536.

Desikan, R.S., Ségonne, F., Fischl, B., Quinn, B.T., Dickerson, B.C., Blacker, D., Buckner, R.L., Dale, A.M., Maguire, R.P., Hyman, B.T., Albert, M.S., Killiany, R.J., 2006. An automated labeling system for subdividing the human cerebral cortex on MRI scans into gyral based regions of interest. Neuroimage 31, 968–980.

Dick, F., Tierney, A.T., Lutti, A., Josephs, O., Sereno, M.I., Weiskopf, N., 2012. In vivo functional and myeloarchitectonic mapping of human primary auditory areas. J. Neurosci. 32, 16095–16105.

Du, J., Younes, L., Qiu, A., 2011. Whole brain diffeomorphic metric mapping via integration of sulcal and gyral curves, cortical surfaces, and images. Neuroimage 56, 162–173.

Eckstein, I., Joshi, A.A., Kuo, C.-C., Leahy, R., Desbrun, M., 2007. Generalized surface flows for deformable registration and cortical matching. Med. Image Comput. Comput. Assist. Interv. 10, 692–700.

Fischl, B., 2004. Automatically parcellating the human cerebral cortex. Cereb. Cortex 14, 11–22.

Fischl, B., Sereno, M.I., Dale, A.M., 1999. Cortical surface-based analysis II: inflation, flattening, and a surface-base coordinate system. Neuroimage 9, 195–207.

Fischl, B., Rajendran, N., Busa, E., Augustinack, J., Hinds, O., Yeo, B.T., Mohlberg, H., Amunts, K., Zilles, K., 2008. Cortical folding patterns and predicting cytoarchitecture. Cereb. Cortex 18, 1973–1980.

Frost, M.A., Goebel, R., 2012. Measuring structural–functional correspondence: spatial variability of specialised brain regions after macro-anatomical alignment. Neuroimage 59, 1369–1381.

Frost, M.A., Goebel, R., 2013. Functionally informed cortex based alignment: an integrated approach for whole-cortex macro-anatomical and ROI-based functional alignment. Neuroimage 83, 1002–1010.

Geyer, S., Weiss, M., Reimann, K., Lohmann, G., Turner, R., 2011. Microstructural parcellation of the human cerebral cortex — from Brodmann's post-mortem map to in vivo mapping with high-field magnetic resonance imaging. Front. Hum. Neurosci. 5, 19.

Glasser, M.F., Van Essen, D.C., 2011. Mapping human cortical areas in vivo based on myelin content as revealed by T1- and T2-weighted MRI. J. Neurosci. 31, 11597–11616.

Glasser, M.F., Goyal, M.S., Preuss, T.M., Raichle, M.E., Van Essen, D.C., 2014. Trends and properties of human cerebral cortex: correlations with cortical myelin content. Neuroimage 93, 165–175.

Goebel, R., Esposito, F., Formisano, E., 2006. Analysis of functional image analysis contest (FIAC) data with brainvoyager QX: from single-subject to cortically aligned group general linear model analysis and self-organizing group independent component analysis. Hum. Brain Mapp. 27, 392–401.

Han, X., Xu, C., Braga-Neto, U., Prince, J.L., 2002. Topology correction in brain cortex segmentation using a multiscale, graph-based algorithm. IEEE Trans. Med. Imaging 21, 109–121.

Han, X., Pham, D.L., Tosun, D., Rettmann, M.E., Xu, C., Prince, J.L., 2004. CRUISE: cortical reconstruction using implicit surface evolution. Neuroimage 23, 997–1012.

Hansen, M.F., Erbou, S., Vester-christensen, M., Larsen, R., Ersbøll, B., Christensen, L.B., 2007. Surface-to-surface registration using level sets. Lect. Notes Comput. Sci. Image Anal. 4522, 780–788.

Hinds, O.P., Rajendran, N., Polimeni, J.R., Augustinack, J.C., Wiggins, G., Wald, L.L., Diana Rosas, H., Potthast, A., Schwartz, E.L., Fischl, B., 2008. Accurate prediction of V1 location from cortical folds in a surface coordinate system. Neuroimage 39, 1585–1599.

Hopf, A., 1955. Über die Verteilung myeloarchitektonischer Merkmale in der isokortikalen Schläfenlappenrinde beim Menschen. J. Hirnforsch. 2, 36–54.

Hopf, A., 1956. Über die Verteilung myeloarchitektonischer Merkmale in der Stirnhirnrinde beim Menschen. J. Hirnforsch. 2, 311–333.

Hopf, A., 1957. Über die Verteilung myeloarchitektonischer Merkmale in de Scheitellappenrinde beim Menschen. J. Hirnforsch. 3, 79–104.

Hurley, A.C., Al-Radaideh, A., Bai, L., Aickelin, U., Coxon, R., Glover, P., Gowland, P.A., 2010. Tailored RF pulse for magnetization inversion at ultrahigh field. Magn. Reson. Med. 63, 51–58.

Jenkinson, M., Bannister, P., Brady, M., Smith, S., 2002. Improved optimization for the robust and accurate linear registration and motion correction of brain images. Neuroimage 17, 825–841.

Joshi, A., Leahy, R., Toga, A.W., Shattuck, D., 2009. A framework for brain registration via simultaneous surface and volume flow. Inf. Process. Med. Imaging 21, 576–588.

Joshi, A.A., Pantazis, D., Li, Q., Damasio, H., Shattuck, D.W., Toga, A.W., Leahy, R.M., 2010. Sulcal set optimization for cortical surface registration. Neuroimage 50, 950–959.

Klein, A., Tourville, J., 2012. 101 labeled brain images and a consistent human cortical labeling protocol. Front. Neurosci. 6, 171.

Klein, A., Andersson, J., Ardekani, B.A., Ashburner, J., Avants, B., Chiang, M.-C., Christensen, G.E., Collins, D.L., Gee, J., Hellier, P., Song, J.H., Jenkinson, M., Lepage, C., Rueckert, D., Thompson, P., Vercauteren, T., Woods, R.P., Mann, J.J., Parsey, R.V., 2009. Evaluation of 14 nonlinear deformation algorithms applied to human brain MRI registration. Neuroimage 46, 786–802.

Koenderink, J.J., van Doorn, A.J., 1992. Surface shape and curvature scales. Image Vis. Comput. 10, 557–564.

Kozinska, D., Tretiak, O.J., Nissanov, J., Ozturk, C., 1997. Multidimensional alignment using the euclidean distance transform. Graph. Model. Image Process. 59, 373–387.

Litke, N., Droske, M., Rumpf, M., Schr, P., 2005. An Image Processing Approach to Surface Matching.

Lüthi, M., Albrecht, T., Vetter, T., 2007. Curvature guided surface registration using level sets. International Congress and Exhibition of Computer Assisted Radiology and Surgery.

Lutti, A., Dick, F., Sereno, M.I., Weiskopf, N., 2014a. Using high-resolution quantitative mapping of R1 as an index of cortical myelination. Neuroimage 93, 176–188.

Lutti, A., Dick, F., Sereno, M.I., Weiskopf, N., 2014b. Using high-resolution quantitative mapping of R1 as an index of cortical myelination. Neuroimage 93 (Pt 2), 176–188.

Marques, J.P., Kober, T., Krueger, G., van der Zwaag, W., Van de Moortele, P.F., Gruetter, R., 2010. MP2RAGE, a self bias-field corrected sequence for improved segmentation and T1-mapping at high field. Neuroimage 49, 1271–1281.

Miller, M.I., 2004. Computational anatomy: shape, growth, and atrophy comparison via diffeomorphisms. Neuroimage 23 (Suppl. 1), S19–S33.

Nieuwenhuys, R., Broere, C.A.J., Cerliani, L., 2014. A new myeloarchitectonic map of the human neocortex based on data from the Vogt–Vogt school. Brain Struct. Funct. http://dx.doi.org/10.1007/s00429-014-0884-8 [Epub ahead of print].

Ono, M., Kubick, S., Abernathey, C.D., 1990. Atlas of the Cerebral Sulci. Thieme Medical Publishers.

Osher, S., Sethian, J.A., 1988. Fronts propagating with curvature-dependent speed: algorithms based on Hamilton–Jacobi formulations. J. Comput. Phys. 79, 12–49.

Pantazis, D., Joshi, A., Jiang, J., Shattuck, D.W., Bernstein, L.E., Damasio, H., Leahy, R.M., 2010. Comparison of landmark-based and automatic methods for cortical surface registration. Neuroimage 49, 2479–2493.

Paragios, N., Rousson, M., Ramesh, V., 2003. Non-rigid registration using distance functions. Comput. Vis. Image Underst. 89, 142–165.

Park, H., Park, J.-S., Seong, J.-K., Na, D.L., Lee, J.-M., 2012. Cortical surface registration using spherical thin-plate spline with sulcal lines and mean curvature as features. J. Neurosci. Methods 206, 46–53.

Perrot, M., Rivière, D., Mangin, J.-F., 2011. Cortical sulci recognition and spatial normalization. Med. Image Anal. 15, 529–550.

Petrović, A., Smith, S.M., Menke, R.A., Jenkinson, M., 2009. Methods for tractography-driven surface registration of brain structures. Med. Image Comput. Comput. Assist. Interv. 12, 705–712.

Pons, J.-P., Hermosillo, G., Keriven, R., Faugeras, O., 2006. Maintaining the point correspondence in the level set framework. J. Comput. Phys. 220, 339–354.

Postelnicu, G., Zollei, L., Fischl, B., 2009. Combined volumetric and surface registration. IEEE Trans. Med. Imaging 28, 508–522.

Rettmann, M.E., Han, X., Xu, C., Prince, J.L., 2002. Automated sulcal segmentation using watersheds on the cortical surface. Neuroimage 15, 329–344.

Robinson, E.C., Jbabdi, S., Glasser, M.F., Andersson, J., Burgess, G.C., Harms, M.P., Smith, S.M., Van Essen, D.C., Jenkinson, M., 2014. MSM: a new flexible framework for Multimodal Surface Matching. Neuroimage 100, 414–426.
Sabuncu, M.R., Singer, B.D., Conroy, B., Bryan, R.E., Ramadge, P.J., Haxby, J.V., 2010. Function-based intersubject alignment of human cortical anatomy. Cereb. Cortex 20, 130–140.
Sereno, M.I., Lutti, A., Weiskopf, N., Dick, F., 2013. Mapping the human cortical surface by combining quantitative T1 with retinotopy. Cereb. Cortex 23, 2261–2268.
Shafee, R., Buckner, R.L., Fischl, B., 2015. Gray matter myelination of 1555 human brains using partial volume corrected MRI images. Neuroimage 105, 473–485 (Elsevier B.V.).
Shen, D., Davatzikos, C., 2002. HAMMER: Hierarchical Attribute Matching Mechanism for Elastic Registration 21, pp. 1421–1439.
Stüber, C., Morawski, M., Schäfer, A., Labadie, C., Wähnert, M., Leuze, C., Streicher, M., Barapatre, N., Reimann, K., Geyer, S., Spemann, D., Turner, R., 2014. Myelin and iron concentration in the human brain: a quantitative study of MRI contrast. Neuroimage 93 (Pt 1), 95–106.
Tardif, C.L., Dinse, J., Schäfer, A., Turner, R., Bazin, P.-L., 2013. Multi-modal surface-based alignment of cortical areas using intra-cortical T1 contrast. Multimodal Brain Image Anal. Lect. Notes Comput. Sci. 8159.
Teeuwisse, W.M., Brink, W.M., Webb, A.G., 2012. Quantitative assessment of the effects of high-permittivity pads in 7 Tesla MRI of the brain. Magn. Reson. Med. 67, 1285–1293.
Tosun, D., Prince, J.L., 2008. A geometry-driven optical flow warping for spatial normalization of cortical surfaces. IEEE Trans. Med. Imaging 27, 1739–1753.
Turner, R., 2013. Where matters: new approaches to brain analysis. In: Geyer, S., Turner, R. (Eds.), Microstructural Parcellation of the Human Cerebral Cortex — From Brodmann's Post-mortem Map to In Vivo Mapping with High-field Magnetic Resonance Imaging. Springer, Berlin Heidelberg, pp. 179–196.
Turner, R., 2014. Comparing like with like: the power of knowing where you are. Brain Connect. 4, 547–557.
Van Atteveldt, N., Formisano, E., Goebel, R., Blomert, L., 2004. Integration of letters and speech sounds in the human brain. Neuron 43, 271–282.
Van Essen, D.C., 2005. A Population-Average, Landmark- and Surface-based (PALS) atlas of human cerebral cortex. Neuroimage 28, 635–662.
Van Essen, D.C., Glasser, M.F., 2014. In vivo architectonics: a cortico-centric perspective. Neuroimage 93, 157–164.
Van Essen, D.C., Ugurbil, K., Auerbach, E., Barch, D., Behrens, T.E.J., Bucholz, R., Chang, A., Chen, L., Corbetta, M., Curtiss, S.W., Della Penna, S., Feinberg, D., Glasser, M.F., Harel, N., Heath, A.C., Larson-Prior, L., Marcus, D., Michalareas, G., Moeller, S., Oostenveld, R., Petersen, S.E., Prior, F., Schlaggar, B.L., Smith, S.M., Snyder, A.Z., Xu, J., Yacoub, E., 2012. The Human Connectome Project: a data acquisition perspective. Neuroimage 62, 2222–2231.
Vemuri, B.C., Ye, J., Chen, Y., Leonard, C.M., 2003. Image Registration Via Level-set Motion: Applications to Atlas-based Segmentation 7, pp. 1–20.
Waehnert, M.D., Dinse, J., Weiss, M., Streicher, M.N., Waehnert, P., Geyer, S., Turner, R., Bazin, P.-L., 2014. Anatomically motivated modeling of cortical laminae. Neuroimage 93, 210–220.
Weiss, M., Geyer, S., Lohmann, G., Trampel, R., Turner, R., 2010. Longitudinal relaxation time T1 as a guide to in-vivo myeloarchitecture. 16th Annual Meeting of the Organization for Human Brain Mapping (Barcelona, Spain).
Yeo, B.T.T., Sabuncu, M.R., Vercauteren, T., Ayache, N., Fischl, B., Golland, P., 2010. Spherical demons: fast diffeomorphic landmark-free surface registration. IEEE Trans. Med. Imaging 29, 650–668.
Zhong, J., Phua, D.Y.L., Qiu, A., 2010. Quantitative evaluation of LDDMM, FreeSurfer, and CARET for cortical surface mapping. Neuroimage 52, 131–141.